Kinetic Characterization of the Chymotryptic Activity of the 20S Proteasome

Ross L. Stein,* Francesco Melandri, and Lawrence Dick

ProScript, Inc.,‡ 38 Sidney Street, Cambridge, Massachusetts 02139

Received September 20, 1995; Revised Manuscript Received January 2, 1996⊗

ABSTRACT: In this paper, we report kinetic studies for the chymotryptic activity of the 20S proteasome. Major observations include the following: (1) Reaction progress curves that are recorded at concentrations of Suc-Leu-Leu-Val-Tyr-AMC greater than about 40 μM are biphasic and characterized by initial velocities that decay by a first-order process to final, steady-state velocities. (2) Also at [Suc-Leu-Leu-Val-Tyr-AMC] > 40 μM, initial and steady-state velocities are smaller than predicted from simple, Michaelis−Menten kinetics. (3) The first-order rate constant for the approach to steady-state has a complex dependence on substrate concentration and decreases sigmoidally as substrate concentration increases. These results indicate that the 20S proteasome is a hysteretic enzyme and is subject to substrate inhibition. To explain these observations we propose a minimal kinetic model with two critical mechanistic features: (1) the 20S proteasome has two cooperative active sites for Suc-Leu-Leu-Val-Tyr-AMC and (2) there are two interconvertible conformers of active 20S proteasome. To probe this mechanism in greater detail, we explored the kinetic mechanism of inhibition of the 20S proteasome-catalyzed hydrolysis of Suc-Leu-Leu-Val-Tyr-AMC by the peptide aldehyde, Ac-Leu-Leu-Nle-H. Our studies reveal a nonlinear dependence of reciprocal steady-state velocity on inhibitor concentration (i.e., parabolic inhibition) as well as a nonlinear dependence of the apparent inhibitor dissociation constant on substrate concentration. Both of these observations are explained by binding of inhibitor at multiple sites on the enzyme. Taken together, the results of this study indicate that the 20S proteasome is a conformationally flexible protein that can adjust to the binding of ligands and that has multiple and cooperative active sites. These results support a view of the proteasome's substrate specificity in which (1) substrates are recognized and hydrolyzed by more than one active site; (2) each active site can bind substrates that possess a variety of P_1 residues; and (3) the P_1 residue plays a relatively minor role as a specificity determinant. Finally, we interpret the results of this study to suggest that, *in vivo*, the 20S proteasome requires conformational plasticity for its interactions with regulatory complexes and, after it has combined with appropriate regulatory complexes, to catalyze hydrolysis of proteins.

The 20S proteasome is a large, multimeric proteolytic enzyme (MW = 700 kDa) found in high concentration in all mammalian cells (Ciechanover, 1994; Goldberg et al., 1995; Hochstrasser, 1995; Peters, 1994; Rechsteiner et al., 1993) and is the catalytic core of the larger 26S proteasome (MW = 2000 kDa) that degrades ubiquitinated proteins (Ciechanover, 1994; Goldberg et al., 1995; Rechsteiner et al., 1993). The 26S proteasome catalyzes the final step of the ubiquitin-proteasome pathway of protein degradation which has been shown to be the principle pathway for intracellular protein turnover (Ciechanover, 1994; Hochstrasser, 1995) and for the regulated degradation of a number of important cellular proteins (Hochstrasser, 1995), such as cyclins (Murray, 1995), tumor suppresser protein p53 (Rolfe et al., 1995; Scheffner et al., 1993; Shkedy et al., 1994), and IκBα (Chen et al., 1995; Palombella et al., 1994).

Early electron microscopic studies revealed that the 20S proteasome resembles a cylinder of four stacked rings, each ring being composed of seven subunits (Peters, 1994; Koster et al., 1995). Additional biochemical studies of eukaryotic proteasomes further revealed the subunit composition to be $\alpha_7\beta_7\beta_7\alpha_7$, in which the seven α-subunits are different but related and the seven β-subunits are different but related (Goldberg et al., 1995; Peters 1994; Koster et al., 1995). Recently, the X-ray crystallographic structure of the 20S proteasome from *Thermoplasma acidophilum* was solved (Lowe et al., 1995) and revealed that the active sites of the enzyme are located in the β-subunits on the inner surface of the cylinder. Furthermore, this enzyme is unique among all proteases in having a threonine residue as its active site nucleophile (Lowe et al., 1995; Seemuller et al., 1995). In addition, this Thr residue is the N-terminal amino acid of the β-subunits (Lowe et al., 1995; Seemuller et al., 1995). Significantly, while the 20S proteasome from *T. acidophilum* has seven identical β-subunits, and thus seven active sites, the 20S proteasome from mammals has only four subunits with N-terminal Thr residues (Seemuller et al., 1995).

A unique feature of the 20S proteasome is its broad P_1[1] specificity (Goldberg et al., 1995). This enzyme has been shown to efficiently hydrolyze peptide substrates such as Suc-Leu-Leu-Val-Tyr-AMC,[2] Z-Leu-Leu-Arg-AMC, and Z-Leu-Leu-Glu-2NA, and hydrolysis of these substrates has been the basis for the definition of chymotryptic, tryptic, and

* To whom correspondence should be addressed.
‡ Formerly MyoGenics, Inc.
⊗ Abstract published in *Advance ACS Abstracts,* March 1, 1996.

[1] The nomenclature for the amino acid residues of the substrate (P_n, ..., P_3, P_2, P_1) and corresponding protease active subsites to which they bind (S_n, ..., S_3, S_2, S_1) is that of Schecter and Berger (1967).

[2] Abbreviations: Suc, *N*-succinyl; AMC, 7-amino-4-methylcoumarin amide; 2NA, 2-naphthyl amide; Z, benzyloxycarbonyl; BrAAP, branched chain amino acid preferring; SNAAP, small neutral amino acid preferring.

0006-2960/96/0435-3899$12.00/0

peptidylglutamyl peptide-hydrolyzing activities of the proteasome, respectively (Goldberg et al., 1995; Orlowski, 1990). In addition, a number of other hydrolytic activities of the proteasome have also been described, such as the BrAAP and SNAAP activities (Orlowski et al., 1993). More recently, studies of protein hydrolysis have revealed that this enzyme's specificity is even broader than previously thought: the 20S proteasome is able to cleave proteins and peptides between virtually any two amino acids (Dick, 1994; Dick et al., 1991; Wenzel et al., 1994). It is still unclear how the various activities are divided among the four active sites of mammalian proteasomes.

The best-characterized peptidase activity of the 20S proteasome is the chymotryptic activity.[3] As part of a program to develop inhibitors of the proteasome, we have targeted this activity for mechanism-based inhibitor design. To this end, we have undertaken a detailed study of the chemical and kinetic mechanism of the chymotryptic activity of the 20S proteasome. In this paper, we report findings that suggest a complex mechanism for the 20S proteasome involving substrate-induced hysteresis (Frieden, 1979; Neet, 1995; Neet & Ainslie, 1980), substrate inhibition, and multiple binding sites for both substrate Suc-Leu-Leu-Val-Tyr-AMC and the peptide aldehyde inhibitor, Ac-Leu-Leu-Nle-H. These results directly impact on our interpretation of the substrate specificity of the proteasome and suggest how this enzyme might be regulated *in vivo*.

EXPERIMENTAL PROCEDURES

General. Buffer salts were purchased from Sigma Chemical Co. Suc-Leu-Leu-Val-Tyr-AMC and Ac-Leu-Leu-Nle-H were purchased from Bachem and Calbiochem, respectively.

Purification of Latent 20 Proteasome from Rabbit Muscle. The 20S proteasome is purified from rabbit psoas muscle according to modification of literature procedures (Ganoth et al., 1988; Hough et al., 1987). Briefly, psoas muscle is excised and sectioned into small pieces and homogenized in buffer A (25 mM Hepes, pH 7.6, 1 mM DTT) at a buffer/wet-weight ratio of 3/1. The homogenate is centrifuged at 10 000*g* for 20 min, and the resulting supernatant is ultracentrifuged at 100 000*g* for 1 h. The supernatant from the ultracentrifugation step is filtered through a 0.2 μm filter and applied to a DE52 anion exchange column equilibrated in buffer A. The column is washed with 5 column volumes of buffer A, and absorbed proteins are eluted with 2.5 volumes of buffer A containing 500 mM NaCl. The eluate (fraction II) is brought to 38% ammonium sulfate saturation and centrifuged at 10 000*g* for 20 min. The supernatant is now brought to 85% ammonium sulfate saturation and centrifuged at 10 000*g* for 20 min. The pellet from this centrifugation was resuspended in a minimal volume of buffer A to produce fraction IIB, which is then dialyzed against 4 L of buffer A. Dialyzed FIIB is applied to a MonoQ anion exchange column and eluted with a 40 column volume gradient of 0−500 mM NaCl. Fractions with SDS-activatable Suc-Leu-Val-Tyr-AMC-hydrolyzing activity are pooled, diluted to a NaCl concentration of 50 mM, and applied to a 1 mL heparin-Sepharose Hi-Trap column. Elution is performed with a 20 column volume gradient from 50 to 500 mM NaCl. Active fractions are pooled and concentrated using a 30 000 MW cutoff Centricon centrifugal concentrator. The concentrate is applied to a Superose 6 size-exclusion chromatography column and eluted with buffer A containing 100 mM NaCl. Fractions with SDS-activatable Suc-Leu-Leu-Val-Tyr-AMC-hydrolyzing activity are analyzed by 12.5% SDS−PAGE, and pooling decisions are made on the basis of purity. This 20S proteasome pool is aliquoted and stored at −80 °C for subsequent use. 20S proteasome prepared in this manner migrates as a single band in non-denaturing PAGE and displays the new diagnostic pattern of bands when subjected to SDS−PAGE (Ganoth et al., 1988; Hough et al., 1987).

Kinetic Methods. In a typical kinetic run, 2.00 mL of assay buffer (20 mM HEPES, 0.5 mM EDTA, 0.035% SDS, pH 7.8) and Suc-Leu-Leu-Val-Tyr-AMC in DMSO were added to a 3 mL fluorescence cuvette, and the cuvette was placed in the jacketed cell holder of a Hitachi 2000 fluorescence spectrophotometer. Reaction temperature was maintained at 37.0 ± 0.02 °C by a circulating water bath. After the reaction solution had reached thermal equilibrium (~5 min), 1−10 μL of the stock enzyme solution was added to the cuvette. Reaction progress was monitored by the increase in fluorescence emission at 440 nm (λ_{ex} = 380 nm) that accompanies cleavage of AMC from peptide-AMC substrates. For each kinetic run, 200−1000 data points, corresponding to {time, FI} pairs, were collected by a microcomputer interfaced to the fluorescence spectrophotometer.

RESULTS

Effect of SDS on Latent 20S Proteasome. In the studies of this manuscript, we wanted to characterize the kinetics of the chymotryptic activity of SDS-activated 20S proteasome. While SDS activation of the proteasome has been described in literature (Dahlmann et al., 1993; Tanaka et al., 1989; Yamada et al., 1995), these reports have generally been qualitative treatments of stopped-time assays and, thus, were not a suitable foundation for the studies we wanted to pursue. We, therefore, undertook a detailed kinetic analysis of the effect of SDS on the 20S proteasome-catalyzed hydrolysis of Suc-Leu-Leu-Val-Tyr-AMC.

The primary data from these experiments are shown in Figure 1 where we plot reaction progress curves for the 20S proteasome-catalyzed hydrolysis of Suc-Leu-Leu-Val-Tyr-AMC at SDS concentrations ranging from 0 to 2.5 mM (0%−0.072%). In the SDS concentration range from 0 to 0.70 mM, we observe activation of latent 20S proteasome (panel A, Figure 1). In this concentration range, proteasome activity increases from a value near zero to a final, steady-state velocity of 1 FU/s that is independent of SDS concentration (panel A, Figure 2). The approach to steady-state is described by a pseudo-first-order rate constant, k_{lag}, that increases with increasing SDS concentration as shown in panel B of Figure 2.

In contrast to this, in the SDS concentration range from 1.1 to 2.5 mM, we observe inactivation of 20S proteasome. In this concentration range, proteasome activation is instan-

[3] In this study, we define the "chymotryptic activity" of the proteasome as the hydrolysis of the Suc-Leu-Leu-Val-Tyr-AMC to produce Suc-Leu-Leu-Val-Tyr and AMC. The original definition of chymotryptic activity was based on hydrolysis of Z-Gly-Gly-Leu-pNA, a substrate with a P_1 leucine residue (Orlowski & Michaud, 1989). Possibly, this activity should have been called the "elastolytic activity" of the proteasome since both human leukocyte and porcine pancreatic elastase but *not* chymotrypsin have a P_1 preference for Leu over Tyr (Stein, 1985).

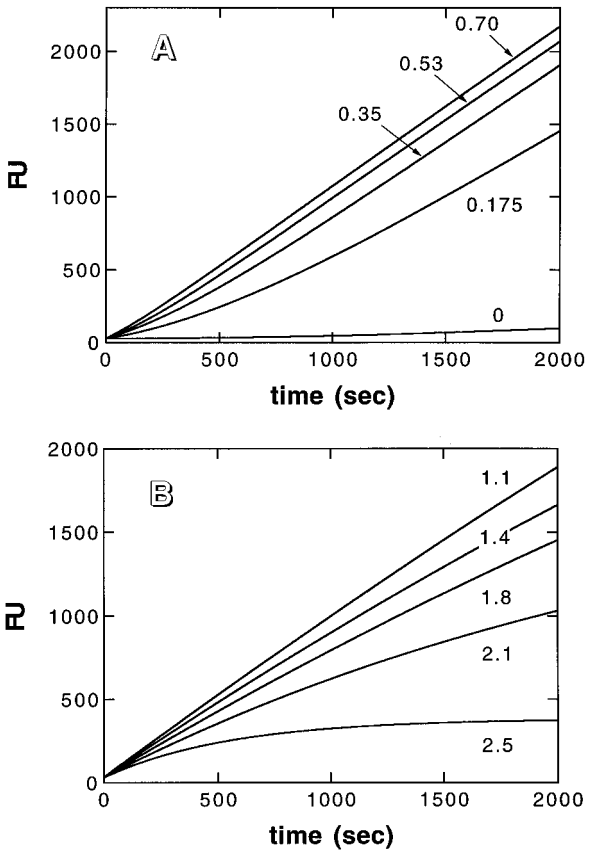

FIGURE 1: Effect of SDS on chymotryptic activity of the 20S proteasome. (A) Progress curves for the activation of latent 20S proteasome by SDS concentrations ranging from 0 to 0.70 mM. (B) Progress curves for the inactivation of latent 20S proteasome by SDS concentrations ranging from 1.1 to 2.5 mM. Reactions were conducted at 37.0 ± 0.02 °C and pH 7.8 in a buffer containing 20 mM HEPES, 0.5 mM EDTA, 4 μM Suc-Leu-Leu-Val-Tyr-AMC, and the indicated amounts of SDS. Progress curves were initiated by the addition of latent 20S proteasome to a final concentration of 0.5 nM.

taneous on the time scale of the experiments (i.e., $v_o \approx 1$ FU/s; panel C, Figure 2) and is followed by [SDS]-dependent inactivation. Inactivation of the proteasome by SDS is a pseudo-first-order process that is described by k_{inact} and depends on SDS concentration as shown in panel D of Figure 2.

On the basis of these results, we chose an SDS concentration of 1.2 mM (0.035%) for the experiments of this study. At 0.035% SDS, proteasome activation occurs in the dead time of the kinetic experiment and progress curves are linear within 5% for at least 1500 s.

Substrate-Induced Hysteresis and Inhibition of the 20S Proteasome. In the course of our experiments, we observed that at concentrations of Suc-Leu-Leu-Val-Tyr-AMC greater than about 30 μM, reaction progress curves become biphasic as illustrated in Figure 3. This departure from linearity cannot be explained by substrate depletion since in these experiments substrate consumption is always less than 5%, as illustrated in Figure 3, nor can this nonlinearity be due to a stoichiometric burst since enzyme concentration in these experiments is on the order of 0.5 nM and the burst amplitude is at least 20-fold greater than this (see Figure 3) and not proportional to enzyme concentration (data not shown). Other trivial explanations (e.g., poor temperature control) were also eliminated. We conclude that this behavior is an example of substrate-induced enzyme hysteresis, a phenomenon in which formation of an enzyme:substrate complex causes the conversion of enzyme from one form to another (Frieden, 1979; Neet, 1995; Neet & Ainslie, 1980). If the conversion is slow relative to substrate turnover and if the two forms of enzyme have different kinetics properties, then pre-steady-state bursts or lags will be observed.

Progress curves for the 20S proteasome-catalyzed hydrolysis of Suc-Leu-Leu-Val-Tyr-AMC are described by eq 1:

$$\text{product} = v_s t + \frac{v_o - v_s}{k_{hys}}\{1 - \exp(-k_{hys} t)\} \qquad (1)$$

where v_s is the steady-state velocity, v_o is the initial velocity, and k_{hys} is a pseudo-first-order rate constant for the approach to steady-state.

As our initial mechanistic probe of the hysteresis that accompanies 20S proteasome catalysis, we sought to understand the substrate concentration-dependence of this process. To this end, we recorded reaction progress curves at substrate concentrations ranging from 4 to 400 μM and analyzed them according to eq 1 to determine how the three experimentally determinable parameters, v_s, v_o, and k_{hys}, depend on the concentration of Suc-Leu-Leu-Val-Tyr-AMC.

The substrate concentration-dependence of k_{hys} is shown in Figure 4 and can be fit to the empirical expression of eq 2 to provide mechanism-independent parameters: $k_1 = (18 \pm 3) \times 10^{-3}$ s^{-1}; $k_2 = (0.96 \pm 0.70) \times 10^{-3}$ s^{-1}; $K_a = 500 \pm 1300$ μM; and $K_b = 11 \pm 32$ μM [$\sum$(residuals)$^2 = 7.2 \times 10^{-6}$ s^{-2}].[4]

$$k_{hys} = \frac{k_1}{1 + \frac{[S]}{K_a} + \frac{[S]^2}{K_a K_b}} + k_2 \qquad (2)$$

Significantly, a poor fit is obtained [i.e., $\sum$(residuals)$^2 \approx 20 \times 10^{-6}$ s^{-2}] if the data are fit to the simpler eq 3 involving a first-order dependence on substrate concentration.

$$k_{hys} = \frac{k_1}{1 + \frac{[S]}{K_a}} + k_2 \qquad (3)$$

Third- and higher-order dependencies on substrate concentration provide no better a fit than does eq 2. Although this is a mechanism-independent analysis, it reveals several interesting features of the substrate concentration-dependence of proteasome hysteresis that will be critical in our development of a mechanistic model: (1) k_{hys} decreases with increasing substrate concentration; (2) k_{hys} has a second-order dependence on substrate concentration. This suggests that two molecules of substrate can bind to the proteasome and influence the hysteresis process; and (3) K_b must be smaller than K_a. This is an example of positive cooperativity in which binding of the first molecule of substrate causes a

[4] Regression analysis of this data set is fairly insensitive to the value of K_a. For example, if we constrain K_a to 100 μM, we obtain the following best-fit parameters: $k_1 = (19 \pm 1) \times 10^{-3}$ s^{-1}; $k_2 = (0.84 \pm 0.67) \times 10^{-3}$ s^{-1}; and $K_b = 31 \pm 11$ μM [$\sum$(residuals)$^2 = 7.4 \times 10^{-6}$ s^{-2}].

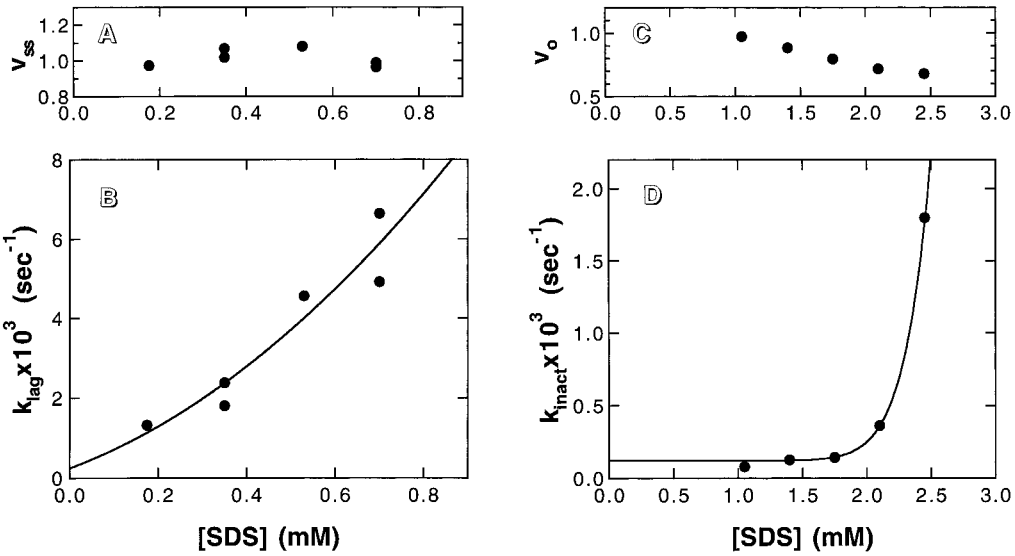

FIGURE 2: Effect of SDS on chymotryptic activity of the 20S proteasome. From the 20S proteasome activation data of Figure 1, values of steady-state velocity (v_{ss}) and first-order rate constant to reach steady-state (k_{lag}) were determined and plotted as a function of [SDS] in A and B, respectively. From the inactivation data of Figure 1, values of initial velocity (v_o) and first-order inactivation rate constants (k_{inact}) were determined and plotted as a function of [SDS] in C and D, respectively. Lines through the data points were drawn using mechanism-independent polynomials and are included to aid the eye. The solid line through the data of panel B is the second-order polynomial, $k_{lag} = 2.4 \times 10^{-3}\ s^{-1} + (4.1 \times 10^{-3}\ mM^{-1}\ s^{-1})[SDS] + (5.6 \times 10^{-3}\ mM^{-2}\ s^{-1})[SDS]^2$, while the solid line through the data of panel D is the high-order polynomial, $k_{inact} = 1.2 \times 10^{-3}\ s^{-1} + (2 \times 10^{-8}\ mM^{-12}\ s^{-1})[SDS]^{12}$.

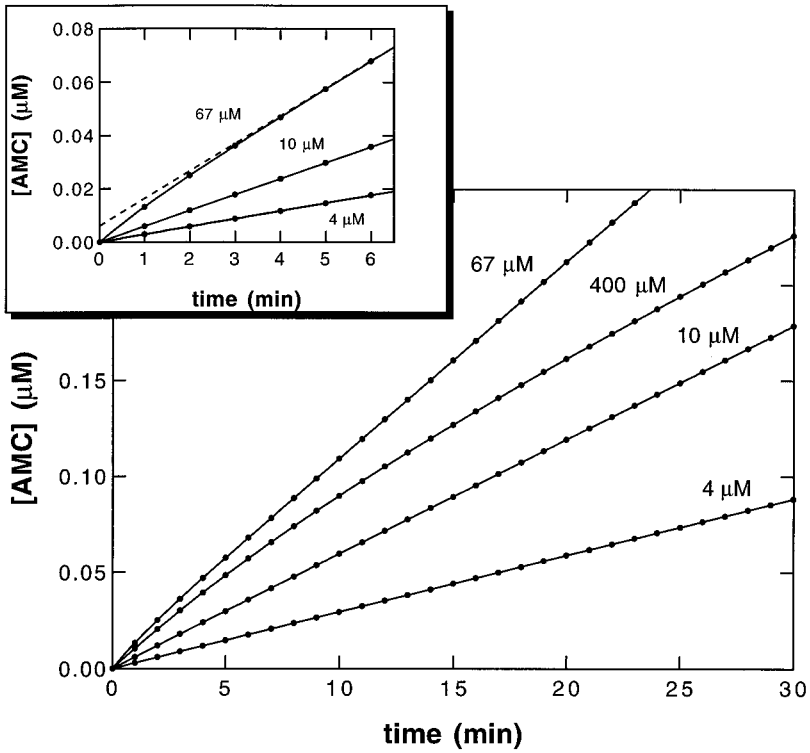

FIGURE 3: Progress curves for the hydrolysis of Suc-Leu-Leu-Val-Tyr-AMC by the 20S proteasome. Reactions were conducted at 37.0 ± 0.02 °C and pH 7.8 in a buffer containing 20 mM HEPES, 0.5 mM EDTA, and 0.035% SDS. Reaction was initiated by the addition of latent 20S proteasome to a final concentration of 0.5 nM. Solid lines through the data for [S] = 4 μM and 10 μM were drawn using a linear relationship of [AMC] on time and slopes (2.95 ± 0.01) × 10^{-3} and (5.97 ± 0.01) × 10^{-3} μM/min, respectively. Solid lines through the data for [S] = 67 and 400 μM were drawn using eq 1 and the following best-fit parameters: $v_o = (14.3 \pm 0.03) \times 10^{-3}$ μM/min, $v_s = (10.3 \pm 0.01) \times 10^{-3}$ μM/min, and $k_{hys} = 0.651 \pm 0.009$ min^{-1}; and $v_o = (10.6 \pm 0.05) \times 10^{-3}$ μM/min, $v_s = (6.08 \pm 0.01) \times 10^{-3}$ μM/min, and $k_{hys} = 0.0942 \pm 0.0013$ min^{-1}, respectively. The inset more clearly illustrates the attainment of steady-state for [S] = 67 μM. The dashed line was drawn with a slope of 10.3 × 10^{-3} μM/min and a *y*-intercept, or burst amplitude, of 6.15 × 10^{-3} μM [= $(v_o - v_s)/k_{hys}$].

conformational change in the proteasome to allow a second substrate to bind more tightly.

We next consider the substrate concentration-dependencies of the initial and steady-state velocities derived from our progress curve analysis. These data are plotted in Figure 5 where we can clearly see that at substrates concentrations greater than about 40 μM, both v_o and v_s are smaller than values predicted from simple Michaelis−Menten kinetics and thus exhibit substrate inhibition. A general solution to parameter estimation for enzyme kinetics that deviate from classic Michaelis−Menten kinetics has been described by Bardsley et al. (1980) and relies on the high-order, phenom-

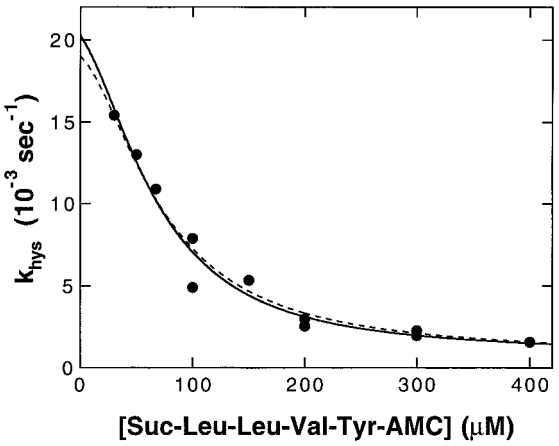

FIGURE 4: Dependence of k_{hys} on substrate concentration for the 20S proteasome-catalyzed hydrolysis of Suc-Leu-Leu-Val-Tyr-AMC. The solid line through the data was drawn using the empirical expression of eq 2 and the best-fit parameters $k_1 = (19 \pm 1) \times 10^{-3}$ s^{-1}, $k_2 = (0.84 \pm 0.67) \times 10^{-3}$ s^{-1}, and $K_b = 31 \pm 11$ μM (K_a constrained to 200 μM). The dashed line through the data was drawn using the expression of eq 15, which is based on the mechanism of Scheme 3 and the parameters $k_\alpha = 14 \times 10^{-3}$ s^{-1}, $k_\beta = 5 \times 10^{-3}$ s^{-1}, $k_\gamma = 0.5 \times 10^{-3}$ s^{-1}, $k_{-\alpha} = 4 \times 10^{-3}$ s^{-1}, $k_{-\beta} = 1 \times 10^{-3}$ s^{-1}, $k_{-\gamma} = 0.1 \times 10^{-3}$ s^{-1}, $K_{se} = K_{se'} = 200$ μM, and $K_{ses} = K_{se's} = 30$ μM.

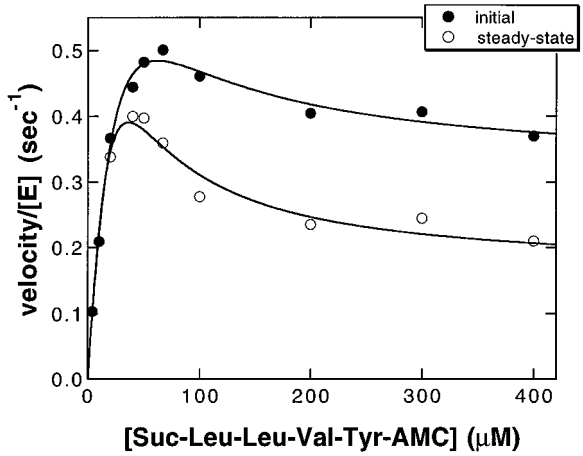

FIGURE 5: Dependence of initial and steady-state velocity on substrate concentration for the 20S proteasome-catalyzed hydrolysis of Suc-Leu-Leu-Val-Tyr-AMC. Solid line through the data for initial velocities (filled circles) was drawn using eq 5 and the best-fit parameters $\alpha_1 = (2.6 \pm 0.4) \times 10^{-2}$ μM^{-1} s^{-1}; $\alpha_2 = (2.4 \pm 1.1) \times 10^{-4}$ μM^{-2} s^{-1}; $\beta_1 = (2.1 \pm 1.1) \times 10^{2}$ μM^{-1}; and $\beta_2 = (7.6 \pm 2.3) \times 10^{-4}$ μM^{-2}. Solid line through the data for steady-state velocities (open circles) was drawn using eq 5 and the best-fit parameters $\alpha_1 = (2.3 \pm 0.3) \times 10^{-2}$ μM^{-1} s^{-1}; $\alpha_2 = (2.0 \pm 1.1) \times 10^{-4}$ μM^{-2} s^{-1}; $\beta_1 = (0.55 + 0.42) \times 10^{-2}$ μM^{-1}; and $\beta_2 = (12 \pm 5) \times 10^{-4}$ μM^{-2}.

enologic kinetic expression, eq 4:

$$\frac{v_s}{[E]} = \frac{\alpha_1[S] + \alpha_2[S]^2 + ... + \alpha_n[S]^n}{1 + \beta_1[S] + \beta_2[S] + ... + \beta_n[S]^n} \quad (4)$$

The simplest form of eq 4 that can account for the data of Figure 5 occurs with $n = 2$:

$$\frac{v_s}{[E]} = \frac{\alpha_a[S] + \alpha_2[S]^2}{1 + \beta_1[S] + \beta_2[S]^2} \quad (5)$$

When the data set for v_o are fit to this equation by nonlinear least-squares analysis, the following best-fit parameters were obtained: $\alpha_1 = (2.6 \pm 0.4) \times 10^{-2}$ μM^{-1} sec^{-1}; $\alpha_2 = (2.4 \pm 1.1) \times 10^{-4}$ μM^{-2} s^{-1}; $\beta_1 = (2.1 \pm 1.1) \times 10^{-2}$ μM^{-1}; and $\beta_2 = (7.6 \pm 2.3) \times 10^{-4}$ μM^{-2}. And for v_s, the following were obtained: $\alpha_1 = (2.3 \pm 0.3) \times 10^{-2}$ μM^{-1} s^{-1}; $\alpha_2 = (2.0 \pm 1.1) \times 10^{-4}$ μM^{-2} s^{-1}; $\beta_1 = (0.55 \pm 0.42) \times 10^{-2}$ μM^{-1}; and $\beta_2 = (12 \pm 5) \times 10^{-4}$ μM^{-2}.

Scheme 1: General Mechanism for Substrate Inhibition

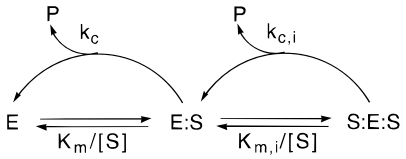

For a simple mechanism of substrate inhibition, such as the one shown in Scheme 1 the following equalities hold:

$$\alpha_1 = \frac{k_c}{K_m} \quad (6)$$

$$\alpha_2 = \frac{k_{c,i}}{K_m K_{m,i}} \quad (7)$$

$$\beta_1 = K_m^{-1} \quad (8)$$

$$\beta_2 = (K_m K_{m,i})^{-1} \quad (9)$$

These equations and the parameter estimates allow us to calculate the mechanistic constants of Scheme 1: $k_c = 1.2$ s^{-1}, $K_m = 48$ μM, $k_c/K_m = 26\,000$ M^{-1} s^{-1}, $k_{c,i} = 0.26$ s^{-1}, and $K_{m,i} = 28$ μM.

Although the mechanism of substrate inhibition that is shown in Scheme 1 is far too simple to explain our observations for the proteasome (see below), this analysis still reveals several interesting features of the proteasome's substrate inhibition that will be important in our development of a mechanistic model: (1) Consistent with our observations for hysteresis, the 20S proteasome can bind two molecules of Suc-Leu-Leu-Val-Try-AMC. (2) Also consistent with our observations for hysteresis, binding of the first molecule of substrate promotes tighter binding of the second. And (3), substrate inhibition of the proteasome is partial; that is, even at high concentrations of Suc-Leu-Leu-Val-Tyr-AMC reaction velocities are not driven to zero but rather decrease and reach a plateau.

Complex Inhibition of the 20S Proteasome by Ac-Leu-Leu-Nle-H. A theme that has been introduced and will be developed below states that catalysis by the 20S proteasome proceeds through a mechanism involving binding and turnover of substrate at multiple sites. To probe this in more detail, we explored the mechanism of inhibition of the proteasome by the peptide aldehyde inhibitor, Ac-Leu-Leu-Nle-H.

In these experiments, we were interested in inhibition of the steady-state reaction by Ac-Leu-Leu-Nle-H; thus, inhibitor was added to a solution of enzyme and substrate that had been allowed to progress into the steady-state. Reaction progress was then monitored for an additional length of time that was sufficient to allow determination of $v_{s,i}$, the steady-state velocity in the presence of inhibitor. We found that at all concentrations of Suc-Leu-Leu-Val-Tyr-AMC and Ac-Leu-Leu-Nle-H, $v_{s,i}$ was attained within the dead-time of our

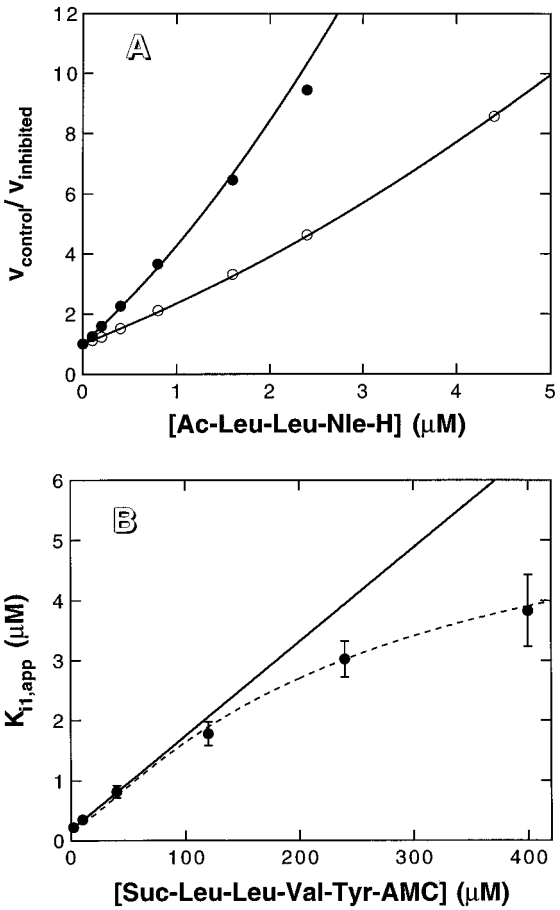

FIGURE 6: Inhibition of the 20S proteasome-catalyzed hydrolysis of Suc-Leu-Leu-Val-Tyr-AMC by Ac-Leu-Leu-Tyr-AMC. Reactions were conducted at 37.0 ± 0.02 °C and pH 7.8 in a buffer containing 20 mM HEPES, 0.5 mM EDTA, and 0.035% SDS. (A) Dixon plots of normalized steady-state velocities for inhibition by Ac-Leu-Leu-Nle-H at substrate concentrations of 10 μM (filled circles) and 40 μM (open circles). Solid lines were drawn according to eq 14 using $K_{i1,app} = 0.35 \pm 0.02$ μM and $K_{i2,app} = 6.4 \pm 2.9$ μM for [S] = 10 μM and using $K_{i1,app} = 0.82 \pm 0.03$ μM and $K_{i2,app} = 10.8 \pm 3.4$ μM for [S] = 40 μM. (B) Dependence of $K_{i1,app}$ on substrate concentration. Solid line was drawn using the expression of eq 11 for simple, competitive inhibition and the parameters $K_i = 0.18$ μM and $K_m = 11$ mM. The dashed line was drawn using eq 21, which is based on the mechanism of Scheme 4 and best-fit parameters $K_{ie} = 0.3 \pm 0.1$ μM, $K_{ses} = 4 \pm 10$ μM, $K_{sei} = 15 \pm 40$ μM, and $K_{ssei} = 300 \pm 110$ μM (K_{se} constrained to 50 μM).

kinetic experiments (i.e., ~20 s). Thus, under our experimental conditions, Ac-Leu-Leu-Nle-H is not a slow-binding inhibitor of the proteasome.[5]

In Figure 6A, we have plotted the inhibitor concentration dependence of $v_s/v_{s,i}$ for substrate concentrations of 10 and 40 μM. These are normalized Dixon plots and, for simple inhibition mechanisms, are linear and adhere to the relationship

$$\frac{v_s}{v_{s,i}} = 1 + \frac{[I]}{K_{i,app}} \tag{10}$$

where for a competitive inhibitor,

$$K_{i,app} = K_i\left(1 + \frac{[S]}{K_m}\right) \tag{11}$$

However, the curvature of these plots suggests parabolic inhibition, which obeys the expression

$$\frac{v_s}{v_{s,i}} = 1 + \frac{[I]}{K_{i1,app}} + \frac{[I]^2}{K_{i1,app}K_{i2,app}} \tag{12}$$

The minimal mechanism for parabolic is shown in Scheme 2 and involves the binding of two molecules of inhibitor to the enzyme.

The dependence of $v_{s,i}$ on inhibitor concentration was determined for substrate concentrations ranging from 2 to 400 μM. At each substrate concentration, the data set was fit by nonlinear least-squares to eqs 13 and 14, which are nonlinearized forms of eqs 10 and 12 for simple competitive and parabolic inhibition, respectively.

$$v_{s,i} = \frac{v_s}{1 + \dfrac{[I]}{K_{i,app}}} \tag{13}$$

$$v_{s,i} = \frac{v_s}{1 + \dfrac{[I]}{K_{i1,app}} + \dfrac{[I]^2}{K_{i1,app}K_{i2,app}}} \tag{14}$$

Table 1 summarizes the parameter estimates. From a visual inspection of Figure 6A and comparing the sum of squares of residuals for the two models, it is clear that the data, at all substrate concentrations, are better fit using the model for parabolic inhibition.

The dependence of $K_{i1,app}$ on substrate concentration is shown in Figure 6B and, in general, indicates that at lower substrate concentrations $K_{i1,app}$ values become smaller. The solid line assumes a model of simple competitive inhibition and uses eq 11 and a K_{i1} value of 0.18 μM. While this relationship adequately describes the data at substrate concentrations below about 100 μM, higher concentrations of substrate fall below the line and thus indicate tighter binding of inhibitor at these substrate concentrations. The underlying mechanism behind this increase in binding affinity is discussed below.

$K_{i2,app}$ also tends toward higher values at higher substrate concentration. However, we believe that any detailed analysis of the substrate concentration-dependence of $K_{i2,app}$ is unwarranted due to the large errors associated with this parameter.

DISCUSSION

Kinetic Model for Proteasome Catalysis and Inhibition. In this section, we describe a model to explain the complex kinetic behavior that accompanies 20S proteasome catalysis and inhibition. We start by considering the 20S proteasome-catalyzed hydrolysis of Suc-Leu-Leu-Val-Tyr-AMC. Two observations that were noted earlier should be restated and bear directly on the kinetic mechanism of this reaction:

• Substrate inhibition is observed for both v_s and v_o. In Figure 5, we see that at substrate concentrations above 40 μM, both initial and steady-state velocities become smaller

[5] Vinitsky et al. (1992) reported that Ac-Leu-Leu-Nle-H is a slow-binding inhibitor of the chymotryptic activity of the 20S proteasome with a final K_i value of 6 μM. The reason for the discrepancy between this study and ours is unclear but may be related to the fact that in their studies unactivated proteasome was used.

Scheme 2: Minimal Mechanism for Parabolic Enzyme Inhibition

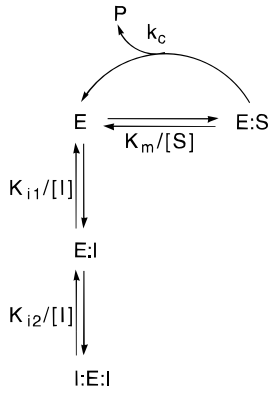

Scheme 3: Mechanism for Substrate-Induced Hysteresis and Inhibition of the 20S Proteasome

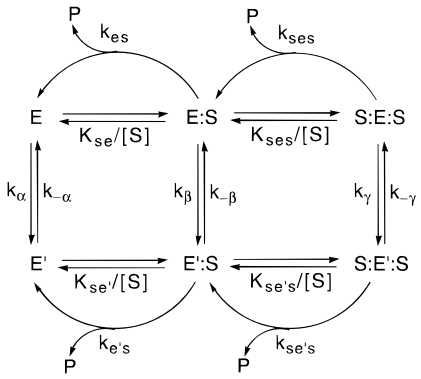

relative to the values that would be predicted on the basis of simple Michaelis−Menten kinetics.

- At high concentrations of substrate, there is clear evidence of hysteresis with initial velocities decaying to the final steady-state velocities. This is clearly seen in Figure 3. Furthermore, as substrate concentration is decreased, k_{hys} increases and v_s approaches and finally equals v_o. That is, at sufficiently low substrate concentrations, reaction velocities do not change over the course of the kinetic experiment.

Thus, any model that we propose must incorporate features of substrate inhibition and substrate-induced hysteresis. The simplest, general model that can accommodate these observations is shown in Scheme 3. In this model, the Michaelis complex, E:S, which forms from combination of enzyme and substrate, can combine with another molecule of substrate to form the ternary complex, S:E:S. This portion of the mechanism is of course identical to Scheme 1 for simple substrate inhibition. Both E:S and S:E:S are catalytically active in Scheme 3, and thus accounts for the partial substrate inhibition that we observe for the proteasome. Hysteresis occurs when any of the various forms of the proteasome are able to slowly convert to other forms. Thus, in the mechanism of Scheme 3, E, E:S, and S:E:S are seen to slowly convert to E′, E′:S, or S:E′:S, respectively. The rate expression that describes the substrate concentration-dependence for the attainment of steady-state for this mechanism is given in eq 15.[6]

$$k_{hys} = \frac{k_\alpha}{1 + \frac{[S]}{K_{se}} + \frac{[S]^2}{K_{se}K_{ses}}} + \frac{k_\beta}{\frac{K_{se}}{[S]} + 1 + \frac{[S]^2}{K_{se}K_{ses}}} + \frac{k_\gamma}{\frac{K_{se}K_{ses}}{[S]^2} + \frac{[S]}{K_{ses}} + 1} + \frac{k_{-\alpha}}{1 + \frac{[S]}{K_{se'}} + \frac{[S]^2}{K_{se'}K_{se's}}} + \frac{k_{-\beta}}{\frac{K_{se'}}{[S]} + 1 + \frac{[S]^2}{K_{se'}K_{se's}}} + \frac{k_{-\gamma}}{\frac{K_{se'}K_{se's}}{[S]^2} + \frac{[S]}{K_{ses}} + 1} \quad (15)$$

Equation 15 is a complex rate expression with eight variable mechanistic parameters and cannot be fit uniquely to the data set of Figure 4. However, mechanistically reasonable sets of parameters can be assigned and have been shown to fit the data quite well. This can be seen in Figure 4 where the dashed line through the data was drawn using eq 15 and the following parameter assignments: $k_\alpha = 14 \times 10^{-3}$ s^{-1}, $k_\beta = 5 \times 10^{-3}$ s^{-1}, $k_\gamma = 0.5 \times 10^{-3}$ s^{-1}, $k_{-\alpha} = 4 \times 10^{-3}$ s^{-1}, $k_{-\beta} = 1 \times 10^{-3}$ s^{-1}, $k_{-\gamma} = 0.1 \times 10^{-3}$ s^{-1}, $K_{se} = K_{se'} = 200$ μM, and $K_{ses} = K_{se's} = 30$ μM. For comparison, we also include the solid line through the data which was drawn according to the empirical expression of eq 2 and the best-fit parameters $k_1 = (19 \pm 1) \times 10^{-3}$ s^{-1}, $k_2 = (0.84 \pm 0.67) \times 10^{-3}$ s^{-1}, and $K_b = 31 \pm 11$ μM (K_a constrained to 200 μM).

In general, we found that if k_{hys} is to decrease with increasing substrate concentration, then the following condition must be met: $k_\alpha \approx k_{-\alpha} > k_\beta \approx k_{-\beta} > k_\gamma \approx k_{-\gamma}$. This follows from the fact that at low [S], $k_{hys} = k_\alpha + k_{-\alpha}$, while at high [S], $k_{hys} = k_\gamma + k_{-\gamma}$. Furthermore, reasonable fits will be obtained only if $K_{se} \approx K_{se'} > K_{ses} \approx K_{se's}$.

Rate expressions were also derived for initial and steady-state velocities for the mechanism of Scheme 3. In deriving the expression for v_o, we considered that at time zero the enzyme exists in two populations, E and E′. The portion of $[E]_{total}$ that is in either E or E′ is governed by K_α, which is equal to [E]/[E′]. Thus, the observed velocity at time zero is the sum of velocities for the reactions catalyzed by E and E′, respectively. From these considerations, we derive the following rate expression for the initial velocity:

Table 1: Inhibition of the 20S Proteasome-Catalyzed Hydrolysis of Suc-Leu-Leu-Val-Tyr-AMC by Ac-Leu-Leu-Nle-H[a]

	competitive inhibition		parabolic inhibition		
[substrate] (μM)	$K_{i,app}$ (μM)	$10^4 \sum$(residuals)^2	$K_{i1,app}$ (μM)	$K_{i2,app}$ (μM)	$10^4 \sum$(residuals)^2
2	0.21 ± 0.01	19	0.22 ± 0.01	19 ± 7	7
10	0.33 ± 0.01	21	0.35 ± 0.02	6 ± 3	9
40	0.74 ± 0.03	21	0.82 ± 0.03	11 ± 3	5
120	1.6 ± 0.1	17	1.8 ± 0.1	38 ± 11	4
240	2.6 ± 0.1	30	3.0 ± 0.2	35 ± 12	8
400	3.4 ± 0.2	13	3.9 ± 0.6	42 ± 20	3

[a] See text for details of analysis.

$$\frac{v_o}{[E]_{total}} = \frac{K_\alpha}{1+K_\alpha}\left\{\frac{k_{es}[S]}{K_{se}+[S]\left(1+\frac{[S]}{K_{ses}}\right)}+\frac{k_{ses}[S]}{K_{ses}\left(1+\frac{K_{se}}{[S]}\right)+[S]}\right\}+\frac{1}{1+K_\alpha}\left\{\frac{k_{e's}[S]}{K_{se}+[S]\left(1+\frac{[S]}{K_{se's}}\right)}+\frac{k_{se's}[S]}{K_{se's}\left(1+\frac{K_{se}}{[S]}\right)+[S]}\right\} \quad (16)$$

Accurate parameter estimates for eq 16 can only be obtained if we know the portion of proteasome in E and E′. Although analysis of the hysteresis data suggests that $K_\alpha < 1$ (note that $K_\alpha = [E]/[E'] = k_{-\alpha}/k_\alpha$), this is not a sufficiently accurate estimate of K_α to allow a unique solution of eq 16. Note, however, that if the proteasome exists predominantly in either E or E′ at time zero, then eq 16 collapses exactly to the simple expression of eq 5 and the parameter estimates that were obtained using eq 5 still hold. Also, for any value of K_α, the initial velocity is simply the algebraic sum of two weighted expressions of the type represented by eq 5. Thus, eq 16 and the mechanism of Scheme 3 can account for the initial velocity data of Figure 5.

Once the steady-state is attained, turnover of substrate takes place from within four complexes: E:S, S:E:S, E′:S, and S:E′:S. On the basis of this consideration, the following rate expression can be derived for the steady-state velocity:

$$\frac{v_s}{[E]_{total}} = \frac{k_{es}[S]}{K_{se}\left(1+\frac{1}{K_\alpha}\right)+[S]\left\{\left(1+\frac{1}{K_\beta}\right)+\frac{[S]}{K_{ses}}\left(1+\frac{1}{K_\gamma}\right)\right\}}+\frac{k_{ses}[S]}{K_{ses}\left\{\left(1+\frac{1}{K_\beta}\right)+\frac{K_{se}}{[S]}\left(1+\frac{1}{K_\alpha}\right)\right\}+[S]\left(1+\frac{1}{K_\gamma}\right)}+\frac{k_{e's}[S]}{K_{se'}(1+K_\alpha)+[S]\left\{(1+K_\beta)+\frac{[S]}{K_{se's}}(1+K_\gamma)\right\}}+\frac{k_{se's}[S]}{K_{se's}\left\{(1+K_\beta)+\frac{K_{se'}}{[S]}(1+K_\alpha)\right\}+[S](1+K_\gamma)} \quad (17)$$

In eq 17,

$$K_\alpha = \frac{k_{-\alpha}}{k_\alpha} = \frac{[E]}{[E']} \quad (18)$$

$$K_\beta = \frac{k_{-\beta}}{k_\beta} = \frac{[E:S]}{[E':S]} \quad (19)$$

$$K_\gamma = \frac{k_{-\gamma}}{k_\gamma} = \frac{[S:E:S]}{[S:E':S]} \quad (20)$$

Equation 17 has eleven variable mechanistic parameters and clearly cannot be solved uniquely for the data set of Figure 5. Furthermore, there is no obvious relationship between the empirical parameters of eq 5 and the mechanistic parameters of eq 17. However, again from our analysis of the hysteresis data and the parameter estimates for eq 15, we can calculate from eqs 18−20 that $K_\alpha \approx K_\beta \approx K_\gamma \approx 0.25$. If this equality is substituted into eq 17, it simplifies to a form that is identical to eq 16, which we have already seen is able to account for our data.

We see that both the hysteresis and substrate inhibition data for the 20S proteasome can be accounted for by the mechanism of Scheme 3. Critical features of the mechanism include two binding sites for substrate and interconvertible conformers of active enzyme.

The inhibition data for the interaction of Ac-Leu-Leu-Nle-H with the 20S proteasome is also consistent with a mechanism involving multiple binding sites for substrate and inhibitor. For Ac-Leu-Leu-Nle-H, we see parabolic inhibition (Figure 6A) as well as a nonlinear dependence $K_{i1,app}$ on substrate concentration (Figure 6B). Both of these observations can only be explained by binding of inhibitor at multiple sites on the enzyme. What we cannot tell from kinetic data is whether the sites to which Ac-Leu-Leu-Nle-H binds are the same as the sites to which Suc-Leu-Leu-Val-Tyr-AMC binds.

To explain the nonlinear dependence of $K_{i1,app}$ on substrate concentration, we propose the mechanism of Scheme 4.[7] Here we see that at very low substrate concentration, where the predominant form of enzyme is E, inhibitor binds to form E:I. As substrate is increased and E:S begins to accumulate, I:E:S also forms. And finally, at very high substrate where S:E:S has formed, Ac-Leu-Leu-Nle-H can also bind to form S:E:S:I. The dependence of $K_{i1,app}$ on substrate concentration for this mechanism is given in eq 21.

$$K_{i1,app} = K_{ie}\left(\frac{1+\frac{[S]}{K_{se}}+\frac{[S]^2}{K_{se}K_{ses}}}{1+\frac{[S]}{K_{sei}}+\frac{[S]^2}{K_{sei}K_{ssei}}}\right) \quad (21)$$

The dashed line of Figure 6B was drawn using this equation and the following best-fit parameters: $K_{ie} = 0.3 \pm 0.1$ μM, $K_{ses} = 4 \pm 10$ μM, $K_{sei} = 15 \pm 40$ μM, and $K_{ssei} = 300 \pm 110$ μM. In this exercise, K_{se} was constrained to 50 μM, a value that is consistent with our previously determined values for this constant (see above). From these parameters and the mechanism of Scheme 4, we can also calculate $K_{ies} =$

[6] In this paper, rate constant nomenclature is according to the following rules: (1) First-order catalytic constants have subscripts that correspond to the complex that is turning over. Thus, k_{es} is the first-order rate constant for the turnover of the Michaelis complex E:S. (2) Dissociation constants have subscripts that correspond to the complex that is dissociating; the first letter of the subscript refers to the substance that is dissociating from the enzyme complex. Thus, K_{ses} is the dissociation constant for the breakdown of S:E:S to E:S and S.

[7] For simplicity, this mechanism describes the situation at relatively low concentrations of inhibitor where the binding manifold that is governed by the composite constant $K_{i1,app}$ obtains. Also, for simplicity's sake, this mechanism only considers the steady-state situation. Thus, each enzyme species that is shown in Scheme 4 must be regarded as a weighted average of the several species that are present at steady-state.

Scheme 4: Mechanism for Multisite Inhibition of the Proteasome

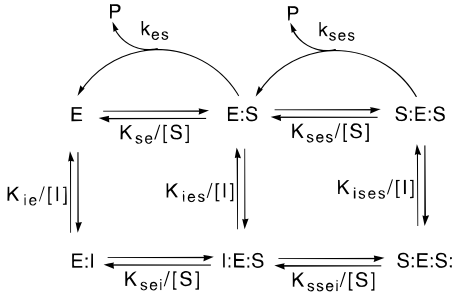

0.1 μM and $K_{ises} = 7$ μM. Binding of Ac-Leu-Leu-Nle-H to E:S is tighter than to free enzyme but of reduced affinity to the ternary complex, S:E:S.

P_1 Specificity of the 20S Proteasome and the Existence of Multiple, Cooperative Active Sites. Quite apart from its detailed kinetic analysis, our work supports earlier, qualitative studies (Djaballah & Rivett, 1992; Djaballah et al., 1993; Figueiredo-Pereira et al., 1995; Orlowski et al., 1991) that established the cooperative nature of proteasome catalysis. Taken together, these studies indicate that a given peptide substrate or inhibitor can bind to multiple active sites or regulatory sites on the proteasome. The existence of multiple binding sites for a single peptide directly impacts on how we should interpret one of the most intriguing features of the proteasome: its broad P_1 specificity.

At last count, nine peptidase activities have been described for eukaryotic 20S proteasomes: the major tryptic (Orlowski & Michaud, 1989), a second tryptic (Arribas & Castano, 1990), the major chymotryptic (Orlowski & Michaud, 1989), a second chymotryptic (Djaballah et al., 1992), an acidic chymotryptic (Figueiredo-Pereira et al., 1995), a low-affinity peptidylglutamyl peptide-hydrolyzing (Orlowski & Michaud, 1989), a high-affinity peptidylglutamyl peptide-hydrolyzing (Djaballah & Rivett, 1992; Orlowski et al., 1991), a BrAAP (Orlowski et al., 1993), and a SNAAP (Orlowski et al., 1993). Furthermore, studies with protein and long peptide substrates indicate that the 20S proteasome is able to cleave between nearly any two amino acids (Dick et al., 1991, 1994; Wenzel et al., 1994).

The canonical view of proteasome catalysis states that each activity is associated with one of the 14 distinct subunits of the proteasome (Orlowski et al., 1993; Cardozo, 1993; Djaballah, 1993). However, given that the proteasome contains only four active sites per ring of β-subunits (Seemuller et al., 1995), it is clear that *more than a single type of peptidase activity must reside at a single active site*. We propose that a given substrate is recognized, bound, and hydrolyzed by each active site. Thus, the observed reaction velocity for hydrolysis of a substrate equals the summation over all velocities for the four active sites:

$$v_{obs} = \sum_{\beta=1}^{4} v_\beta = \sum_{\beta=1}^{4} \frac{V_{max,\beta}[S]}{K_{m,\beta} + [S]} \qquad (22)$$

Implicit in this model is that each of the four active sites possess a substrate specificity that overlaps, at least to some degree, with the specificity of the other active sites.[8]

Furthermore, it is becoming increasingly clear that the P_1 residue is *not* the main determinant of substrate specificity for the proteasome (Dick et al., 1994). For example, the aldehyde inhibitor chymostatin has a Phe at P_1 but inhibits equally well the chymotryptic and tryptic activities of the proteasome (Djaballah et al., 1992). Also, Ac-Leu-Leu-Nle-H and Z-Leu-Leu-Leu-H both inhibit the peptidylglutamyl peptide cleaving activity of the proteasome only 5-fold worse than the chymotryptic activity (unpublished results of the authors). Another intriguing observation that bears on the inadequacy of the P_1 residue as a descriptor of substrate specificity, is that Ac-Leu-Leu-Arg-H, an inhibitor of the tryptic activity of the proteasome, potently inhibits cleavage of oxidized insulin B chain at the Gln^4-His^5 (Dick et al., 1991). The composite of data now clearly indicates that the substrate specificity of the proteasome is determined by a complex interplay of binding interactions at active site subsites more distant than S_1.

Physiologic Significance of Substrate Inhibition and Hysteresis for the 20S Proteasome. We have seen that these studies document complex kinetic behavior for the 20S proteasome-catalyzed hydrolysis of Suc-Leu-Leu-Val-Tyr-AMC and for the inhibition of this activity by Ac-Leu-Leu-Nle-H. To explain these results, we propose a kinetic mechanistic model involving multiple, catalytically competent forms of the enzyme and multiple binding/catalytic sites for ligands. Reflection on these results and their mechanistic interpretation begs the following questions: Are these observations a general feature of proteasome catalysis? And, do these observations and the proposed mechanism relate to anything that might be observed *in vivo*? We believe that the answers to these question are yes: These phenomena are general for proteasome catalysis and not restricted to a single substrate and inhibitor nor even to rabbit muscle 20S proteasome. And, perhaps more importantly, the kinetic behavior we have observed does indeed teach us important lessons about how the proteasome might function in nature.

Consider the following points that relate to the general nature of these complex kinetic phenomena:

(1) This behavior is not restricted to hydrolysis of Suc-Leu-Leu-Val-Tyr-AMC. Both Orlowski's and Rivett's groups (Djaballah & Rivett, 1992; Djaballah et al., 1993; Orlowski et al., 1991) have reported cooperative effects during 20S proteasome-catalyzed hydrolysis of Z-Leu-Leu-Glu-βNA.[9] Similarly, we have observed substrate-induced hysteresis and substrate inhibition for both v_o and v_s for the hydrolysis of Z-Leu-Leu-Glu-βNA and Z-Leu-Leu-Glu-AMC by the 20S proteasome (unpublished observations of the authors).

(2) This behavior is not restricted to inhibition by Ac-Leu-Leu-Nle-H. Wilk and co-workers (Figueiredo-Pereira

[8] It is clear from this work, however, that eq 22 is an oversimplification of any kinetic mechanism for the proteasome. Any attempt to derive an accurate kinetic expression for the proteasome will have to include interaction parameters to account for the proteasome's cooperativity. Equation 22 clearly does not acknowledge that the proteasome is an allosteric enzyme.

[9] The studies from Orlowski's (Orlowski et al., 1991) and Rivett's (Djaballah & Rivett, 1992; Djaballah et al., 1993) groups were both conducted using stopped-time assays, and it is, therefore, unfortunately not clear if their results relate to pre-steady-state or steady-state conditions. Mechanistic interpretation of these results is therefore problematic.

[10] Interestingly, Wilk and co-workers (Figueiredo-Pereira et al., 1995) also observed that Z-Ile-Glu(OtBu)-Ala-2-amino-(1-isohexanol), the reduced alcohol analog of Z-Ile-Glu(OtBu)-Ala-Leu-H, *activates* the chymotryptic activity of the 20S proteasome. This observation is consistent with the proteasome having multiple binding sites as we have suggested herein.

et al., 1995) have recently described the inhibition of an "acidic chymotrypsin-like activity" of the 20S proteasome by Z-Ile-Glu(OtBu)-Ala-Leu-H and stated that K_i values could not be determined because the Dixon plots were curvilinear, presumably due to multiple binding sites for the inhibitor.[10] We also see parabolic inhibition of the proteasome by Z-Leu-Leu-Leu-H and other inhibitors (unpublished observations of the authors).

(3) Substrate-induced hysteresis and inhibition is observed not only for the rabbit muscle 20S proteasome that we report here but also during catalysis by 20S proteasome isolated from rabbit reticulocytes and goat erythrocytes (unpublished observations of the authors). Furthermore, pre-steady-state transients have been observed for the ATP-stimulated, 26S proteasome-catalyzed hydrolysis of Suc-Leu-Leu-Val-Tyr-AMC, Z-Leu-Leu-Glu-AMC, and Z-Leu-Val-Arg-AMC (Dahlmann et al., 1995; unpublished observations of the authors). Thus, the existence of multiple binding sites and their complex interactions is not restricted to the 20S proteasome but extends to the physiologically more relevant species, the 26S proteasome.

Thus, several laboratories have now demonstrated that both the 20S and 26S proteasomes have multiple and cooperative binding sites for low molecular weight substrates and inhibitors. The general nature of this behavior justifies consideration of the second question regarding what these phenomena might mean when we consider the proteasome in its *in vivo* setting.

The observations of hysteresis and cooperativity indicate that the 20S proteasome is a conformationally flexible protein. This enzyme undergoes both spontaneous and ligand-induced conformational changes (see Scheme 3). *In vivo*, conformational plasticity of this sort may serve two distinct roles: to allow the 20S proteasome to productively interact with regulatory complexes (DeMartino & Slaughter, 1993) and to allow the subtle adjustments of active site geometries that are required for stabilization of catalytic transition states during substrate hydrolysis.

The existence of cooperativity for the proteasome suggests that when a segment of protein binds to an active site, the occupation of that site is communicated to other active sites to modulate their activity. This communication may be crucial to a correctly choreographed disassembly of a long polypeptide chain that has been fed into the central chamber of the proteasome (Goldberg et al., 1995; Lowe et al., 1995). Only with detailed kinetic and structural studies with protein substrates will we be able to understand all the intricacies of the proteasome's catalytic mechanism.

REFERENCES

Arribas, J., & Castano, J. (1990) *J. Biol. Chem. 265*, 13969−13973.

Bardsley, W. G., Leff, P., Kavanagh, J., & Waight, R. D. (1980) *Biochem. J. 187*, 739−765.

Cardozo, C. (1993) *Enzyme Protein 47*, 296−305.

Chen, Z., Hagler, J., Palombella, V. J., Melandri, F., Scherer, D., Ballard, D., & Maniatis, T. (1995) *Genes Dev. 9*, 1586−1597.

Ciechanover, A. (1994) *Cell 79*, 13−21.

Dahlmann, B., Becher, B., Sobek, A., Ehlers, C., Kopp, F., & Kuehn, L. (1993) *Enzyme Protein 47*, 274−284.

Dahlmann, B., Kuehn, L., & Reinauer, H. (1995) *Biochem. J. 309*, 195−202.

Demartino, G. N., & Slaughter, C. A. (1993) *Enzyme Protein 47*, 314−324.

Dick, L. R., Moomaw, C. R., DeMartino, G. N., & Slaughter, C. A. (1991) *Biochemistry 30*, 2725−2734.

Dick, L. R., Aldrich, C., Jameson, S. C., Moomaw, C. R., Pramanik, B. C., Doyle, C. K., DeMartino, G. N., Bevan, M. J., Forman, J. M., & Slaughter, C. A. (1994) *J. Immunol. 152*, 3884−3894.

Djaballah, H., & Rivett, A. J. (1992) *Biochemistry 31*, 4133−4141.

Djaballah, H., Harness, J. A., Savory, P. J., & Rivett (1992) *Eur. J. Biochem. 209*, 629−634.

Djaballah, H., Rowe, A. J., Harding, S. E., & Rivett, A. J. (1993) *Biochem. J. 292*, 857−862.

Figueiredo-Pereira, M. E., Chen, W.-E., Yuan, H.-M., & Wilk, S. (1995) *Arch. Biochem. Biophys. 317*, 69−78.

Frieden, C. (1979) *Annu. Rev. Biochem. 48*, 471−489.

Ganoth, D., Leshinsky, E., Eytan, E., & Hershko, A. (1988) *J. Biol. Chem. 263*, 12412−12419.

Goldberg, A. L., Stein, R. L., & Adams, J. (1995) *Chem. Bio.* (*in press*).

Hochstrasser, M. (1995) *Current Opinion Biol. 7*, 215−223.

Hough, R., Pratt, G., & Rechsteiner, M. (1987) *J. Biol. Chem. 262*, 8303−8313.

Koster, A. J., Wlaz, J., Lupas, A., & Baumeister, W. (1995) *Mol. Biol. Rep. 21*, 11−20.

Lowe, J., Stock, D., Jap, B., Swickl, P., Baumeister, W., & Huber, R. (1995) *Science 268*, 533−539.

Murray, A. (1995) *Cell 81*, 149−152.

Neet, K. E. (1995) *Methods Enzymol. 249*, 519−567.

Neet, K. E., & Ainslie, G. R. (1980) *Methods Enzymol. 64*, 192−226.

Orlowski, M. (1990) *Biochemistry 29*, 10289−10297.

Orlowski, M., & Michaud, C. (1989) *Biochemistry 28*, 9270−9278.

Orlowski, M., Cardozo, C., Hidalgo, M. C., & Michaud, C. (1991) *Biochemistry 30*, 5999−6005.

Orlowski, M., Cardozo, C., & Michaud, C. (1993) *Biochemistry 32*, 1563−1572.

Palombella, V. J., Rando, A. L., Goldberg, A. L., & Maniatis, T. (1994) *Cell 78*, 773−785.

Peters, J.-M. (1994) *Trends Biochem. Sci. 19*, 377−382.

Rechsteiner, M., Hoffman, L., & Dubiel, W. (1993) *J. Biol. Chem. 268*, 6065−6068.

Rolfe, M., Beer-Romero, P., Glass, S., Eckstein, J., Berdo, I., Theodoras, A., Pagano, M., & Draetta, G. (1995) *Proc. Natl. Acad. Sci. U.S.A. 92*, 3264−3268.

Schecter, I., & Berger, A. (1967) *Biochem. Biophys. Res. Commun. 27*, 157−162.

Scheffner, M., Huibregste, J. M., Vierstra, R. D., & Howley, P. M. (1993) *Cell 75*, 495−505.

Seemuller, E., Lupas, A., Stock, D., Lowe, J., Huber, R., & Baumeister, W. (1995) *Science 368*, 579−581.

Shkedy, D., Gonen, H., Bercovich, B., & Ciechanover, A. (1994) *FEBS Lett. 348*, 126−130.

Stein, R. L. (1985) *Arch. Biochem. Biophys. 236*, 677−680.

Tanaka, K., Yoshimurs, T., & Ichihara, A. (1989) *J. Biochem. 106*, 495−500.

Vinitsky, A., Michaud, C., Powers, J. C., & Orlowski, M. (1992) *Biochemistry 31*, 9421−9428.

Wenzel, T., Eckerskorn, C., Lottspeich, F., & Baumeister, W. (1994) *FEBS Lett. 349*, 20−209.

Yamada, S., Hojo, K., Yoshimura, Y., & Ishikawa, K. (1995) *J. Biochem. 117*, 1162−1169.

BI952262X